On the Nuclear Modification Factor at RHIC and LHC

Andrey Kormilitzin,[1] Eugene Levin,[1,2] and Amir H. Rezaeian[2]

[1] *Department of Particle Physics, Tel Aviv University, Tel Aviv 69978, Israel*
[2] *Departamento de Física, Universidad Técnica Federico Santa María, Avda. España 1680, Casilla 110-V, Valparaiso, Chile*

(Dated: November 5, 2010)

We show that pQCD factorization incorporated with pre-haronization energy-loss effect naturally leads to flatness of the nuclear modification factor R_{AA} for produced hadrons at high transverse momentum p_T. We consider two possible scenarios for the pre-hadronization: In scenario 1, the produced gluon propagates through dense QCD medium and loses energy. In scenario 2, all gluons first decay to quark-antiquark pairs and then each pair loses energy as propagating through the medium. We show that the estimates of the energy-loss in these two different models lead to very close values and is able to explain the suppression of high-p_T hadrons in nucleus-nucleus collisions at RHIC. We show that the onset of the flatness of R_{AA} for the produced hadron in central collisions at midrapidity is about $p_T \approx 15$ and 25 GeV at RHIC and the LHC energies, respectively. We show that the smallness ($R_{AA} < 0.5$) and the high-p_T flatness of R_{AA} obtained from the k_T factorization supplemented with the Balitsky-Kovchegov (BK) equation is rather generic and it does not strongly depend on the details of the BK solutions. We show that energy-loss effect reduces the nuclear modification factor obtained from the k_T factorization about $30 \div 50\%$ at moderate p_T.

I. INTRODUCTION

The nuclear modification factor (NMF) R_{AA} is defined as

$$R_{AA} \equiv \frac{1}{N_{coll}} \frac{\frac{d^2N_{AA}}{dyd^2p_\perp}}{\frac{d^2N_{NN}}{dyd^2p_\perp}}, \tag{1}$$

where N_{coll} denotes the number of binary collisions in nucleus-nucleus (AA) collisions. The measurements in $Au+Au$ collisions at RHIC showed that the value of R_{AA} is small and constant up to high transverse momentum of produced hadrons in central collisions [1–5], see Fig. 1. At first sight such a behavior at high-p_T contradicts the perturbative QCD (pQCD) factorization theorem [7–11]. Accordingly to the factorization theorem, the inclusive gluonic-jet production cross-section with a large transverse momentum p_T is proportional to $A^2\sigma_{\rm hard} x\, G_p^2(x, p_T)$ which leads to $R_{AA} \to 1$ (see Sec. III for the details). On the other hand in the Color Glass Condensate (CGC) approach due to gluon saturation and the appearance of a new dimensional scale, saturation momentum Q_s [12–16], there is a priori no reason to expect the pQCD factorization theorem to be valid. Indeed, it has been proven [17–22] that the factorization theorem can be replaced by the k_T factorization [23–26] for scatterings of dilute-dilute or dilute-dense system of partons (like deep inelastic scattering with nuclei or scattering of two virtual -photons). For the case of scatterings of dense-dense systems when we have three scales: two saturation momenta for two nuclei and the transverse momentum of produced jet, the k_T factorization has not been proven yet. However, for understanding of the NMF behavior, it is enough to discuss the behavior of the inclusive hadron production at transverse momentum p_T larger than both saturation scales. In this kinematic region, the k_T factorization works [17]. Having this in mind we can assume that the k_T factorization works in all kinematic regions for scattering of dense-dense systems.

Based on the k_T factorization, the inclusive production for gluon (jet) in AA collisions at midrapidity can be calculated from the following equation,

$$\frac{d\sigma}{dy\, d^2p_T}\|_{y=0}, = \frac{2C_F}{\alpha_s 2(2\pi)^3}\frac{1}{x_\perp^2}\int d^2b\, d^2B \int_{-\infty}^{+\infty} dz\, e^{-z}\, J_0\left(e^{\frac{1}{2}z}\, x_\perp\right)\ \nabla_z^2 N_G\Big(z; b\Big)\ \nabla_z^2 N_G\left(z; |\vec{b}-\vec{B}|\right), \tag{2}$$

where p_T and y are the transverse momentum and rapidity of the produced gluon, with notations $z = \ln\left(r^2Q_s^2\right)$, $x_\perp = p_T/Q_s$ and $N_G = 2N - N^2$. We defined $C_F = (N_c^2-1)/2N_c$ where N_c denotes the number of colors and α_s is the strong coupling. The forward dipole-nucleus amplitude N can be obtained via solving the Balitsky-Kovchegov equation (BK)[15]. It is seen that Eq. (2) has $x_\perp$-scaling behavior in the kinematic region that the forward dipole amplitude N has the geometric-scaling property.

Using Eq. (2) we can re-write the NMF in the following form:

$$\text{NMF} \equiv \frac{1}{A^2}\frac{S_A^2}{S_p^2}\frac{\mathcal{T}(x_\perp)}{\mathcal{T}\left(x_\perp \frac{Q_{s,A}}{Q_{s,N}}\right)}, \tag{3}$$

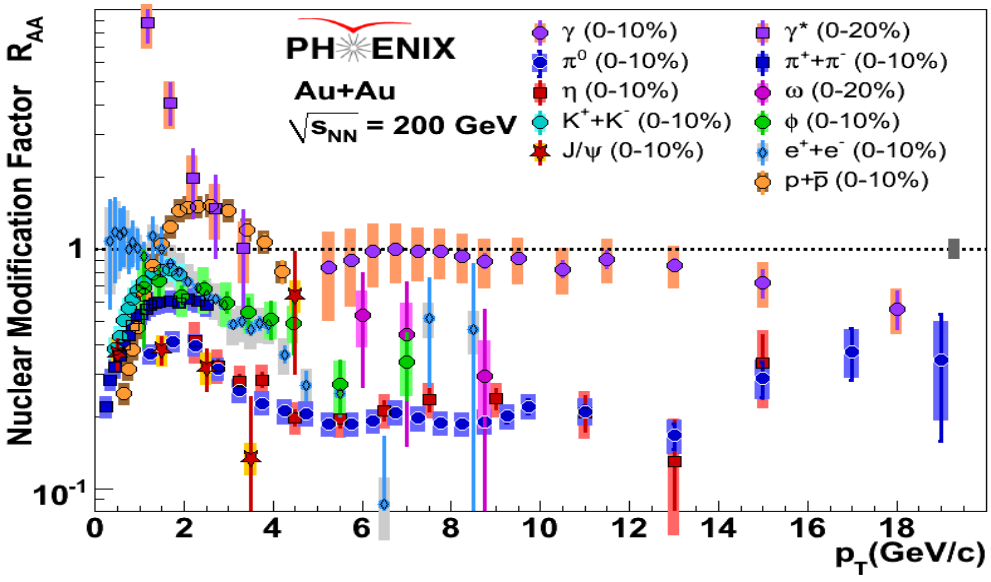

FIG. 1: The NMF for hadrons and direct photon versus transverse momentum p_T in central Au+Au collisions at RHIC. The plot is taken from Ref. [6] from the PHENIX collaboration.

where function $\mathcal{T}$ is defined using Eq. (2). The area of interaction (denoted by S_A and S_p for AA and pp collisions) is well-defined for nucleus-nucleus scatterings while is rather uncertain for proton-proton interactions [27, 28]. In the above for simplicity we assumed that the area of interaction in both AA and and pp collisions can be factorized.

It turns out that the NMF calculated from Eq. (3) is small $R_{AA} < 0.5$ (see Sec IV). Eq. (2) has the geometric scaling behavior which is valid in the saturation region [29] and can be extended to a wider region outside the saturation domain [30]. The geometric scaling behavior is violated for $z^2 > 2\ln\left(Q_s^2(Y)/Q_s(0)\right)$ where $Y = \ln(1/x)$ [30]. Notice that we have $2\ln\left(Q_s^2(Y)/Q_s(0)\right)$ instead of $8\ln\left(Q_s^2(Y)/Q_s(0)\right)$ since $d^2\sigma/d^2p_t \propto N_G^2 \propto N^4$ when N is not small. Therefore, for $z \gg \sqrt{2\ln\left(Q_s^2(Y)/Q_s(0)\right)}$ we expect that the scaling behavior will be broken and the inclusive cross section for jet production for both nucleus-nucleus and proton-proton collisions will be proportional to $\alpha_s(p_T^2)/p_T^4$ and consequently we have $R_{AA} \to 1$. Using the above equation and the saturation scale estimated in Ref. [31] at RHIC energies, one may expect that only for $p_T \leq 3 \div 4\, Q_s$, the NMF to be different from unity. But a slight glance at Fig. 1 shows that this is not the case for inclusive hadrons production for a wide range of p_T while it apparently holds for the production of direct photon [32–34]. Therefore, the small value of the NMF at high p_T may stem from large distance interactions in medium and non-perturbative QCD should be invoked to calculate such interactions [35]. The data on R_{AA} for J/Ψ production supports this conclusion [36–39].

In this paper, we show that the CGC predicts considerable suppression of the NMF at low-p_T both at RHIC and the LHC energies. We will show that based on the CGC prescription at low-p_T, the NMF slowly increases and then flattens at moderate p_T. Based on pQCD, we will then estimate, the onset of the flatness of the NMF at large p_T. The CGC approach is based on classical gluon fields and evolution in leading log(1/x) approximation. In such approximations the energy-loss in processes of gluon emissions is neglected. The systematic approach within pQCD framework [35, 40–45] shows that such emissions alone is not able to describe the experimental values for the NMF and variety of non-perturbative approaches have been developed [45–53]. In this paper, we introduce a simple approach for calculating the energy-loss effect due to pre-hadronization which is able to describe RHIC data at high-p_T. At low-p_T, energy-loss is less important and we show that the CGC prescription Eq. (3) gives rather good description of RHIC data at small Bjorken-x.

In the next section, we calculate the energy-loss effect within two different pre-hadronization pictures. In Sec. III, we discuss the large p_T behavior of the NMF for hadron production at RHIC and the LHC. Sec. IV is devoted to present our numerical results and comparison with the experimental data. As a conclusion, in Sec. IV we highlight our main results.

II. PRE-HADRONIZATION MODELS

Hadronization, unfortunately, could be treated mostly phenomenologically due to our lack of understanding of non-perturbative QCD. There have been several approaches to describe hadronization processes [45–53].

Here, we propose a simple picture for hadronization hoping that the phenomenological uncertainties can be reduced to few parameters which can be then determined from experiment. In our approach, a high energy heavy ion collision can be simplified to three successive stages: 1) parton production 2) pre-hadronization and 3) fragmentation of the produced parton into hadron. At the first stage, we have partons scattering and recombination effects which can be described within the CGC approach. The CGC gives the description of the initial wavefunction of projectiles and the multiple-parton production within a time scale of the order of $1/Q_s$ after collisions. In the second stage, the produced partons propagate and interact with the produced QCD medium and lose energy. Finally, the produced jet subjected to the energy-loss fragments to hadron. Unfortunately, at the moment, only the first stage of hadronization is rather under theoretical control and the last two stages should be modeled. However, the first and the second stages of hadronization determine the main characteristic of the hadron production. We therefore neglect the fragmentation process and instead for simplicity and clarity resort to the Local Parton-Hadron Duality (LPHD) principle [27, 28, 31, 54], namely we assume that the final-state hadronization is a soft process and cannot change the direction of the emitted radiation[1]. Then, the key question is to obtain the fraction of energy of the produced partonic system (in the pre-hadronization stage) which is carried away by hadron, the so-called $z_{A,h}$ parameter. We have recently shown [27] that the data for the inclusive hadron production in pp collisions in a wide range of energies can be described if we assume that the energy loss in the process of fragmentation of the produced gluon into hadron reaches $z_h \approx \frac{1}{2}$. In the following section we calculate the value of z_A in the presence of a dense QCD medium within two different pre-hadronization pictures and we will show that both schemes give rather similar results.

A. Quark-antiquark pre-hadronization model

As a first model, in spirit of all available hadronization models, we assume that hadronization passes a stage in which all gluons first go to quark-antiquark pairs (pre-hadronization)(see Fig. 2). Each pair then decays into hadron in the same way for hadron-hadron, hadron-nucleus and nucleus-nucleus interactions. In such a decay, the fastest hadron carries z_h fraction of energy of the pair.

In nucleus-nucleus interactions, the process of quark-antiquark pair creation is depicted in Fig. 3. In heavy ion collisions, the probability for a gluon with an average transverse momentum Q_{s1} to decay into quark-antiquark ($q\bar{q}$) pair at impact-parameter b with a relative transverse momentum denoted by $\vec{k} \equiv \underline{k}$ ($\underline{k}^2 \equiv k^2$) has the following form[2] [33, 55, 60],

$$
\begin{aligned}
P_{AA}^{q\bar{q}}(y,b,k) \;=\; & \frac{\alpha_s\, Q_{s1}^2}{8\pi^4} \int d^2r \int d^2r'\, e^{-i\frac{1}{2}\underline{k}\cdot(\underline{r}-\underline{r'})} \left\{ \frac{1}{2}\frac{\underline{r}\cdot\underline{r'}}{rr'}\, K_1(rQ_{s1})\, K_1(r'Q_{s1}) + K_0(rQ_{s1}) K_0(r'Q_{s1}) \right\} \\
\times \; & \frac{8\, C_F}{\pi^2\alpha_s} \left\{ \frac{1}{r^2} \left(1 - e^{-\frac{1}{8}\underline{r}^2 Q_{s1}^2}\right) \left(1 - e^{-\frac{1}{8}\underline{r}^2 Q_{s2}^2}\right) + \frac{1}{r'^2} \left(1 - e^{-\frac{1}{8}\underline{r'}^2 Q_{s1}^2}\right) \left(1 - e^{-\frac{1}{8}\underline{r'}^2 Q_{s2}^2}\right) \right. \\
& \left. - \; \frac{1}{(\underline{r}-\underline{r'})^2} \left(1 - e^{-\frac{1}{8}(\underline{r}-\underline{r'})^2 Q_{s1}^2}\right) \left(1 - e^{-\frac{1}{8}(\underline{r}-\underline{r'})^2 Q_{s2}^2}\right) \right\}. \qquad (4)
\end{aligned}
$$

The factor in the first curly bracket is the probability that a gluon decays into quark-antiquark pair $|\Psi_{G\to q\bar{q}}|^2$ (see Fig. 3). This gluon has typical transverse momentum Q_{s1}. The formula is written in the laboratory frame where the nucleus A_2 is at rest. Eq. (4) is derived as a sum of all possible inelastic interactions. For example, for one inelastic interaction with nucleus A_2 the contribution to Eq. (4) has the following form,

$$
\int dz_1 e^{-\frac{1}{2}\sigma(Y,r)\,\rho z_1}\, \rho\, \sigma_{in} e^{-\frac{1}{2}\sigma(Y,r)\,\rho(2R_{A_2}-z_1)}\, e^{-\frac{1}{2}\sigma(Y,r)\,\rho 2R_{A_1}}\; e^{-\frac{1}{2}\sigma(Y,r')\,\rho(2R_{A_2}-z_1)}\, e^{-\frac{1}{2}\sigma(Y,r')\,\rho z_1}, \qquad (5)
$$

where ρ is the nucleon density and R_{A_i} is the radius of the nucleus A_i. Eq. (5) indicates that a dipole with a transverse size r interacts inelastically with the nucleon located at point x_1 in nucleus A_2 and exponents provide that no inelastic

[1] The same idea was used in the KLN [31] and the LR [28] approaches which describes the rapidity distribution of heavy-ion collisions data in a wide range of energies. This scheme also describes experimental data from e^+e^- annihilation into hadrons [54] and inclusive hadron productions in pp collisions including the recent LHC data [27].

[2] The derivation is based on the approaches suggested in Refs. [17, 56–59].

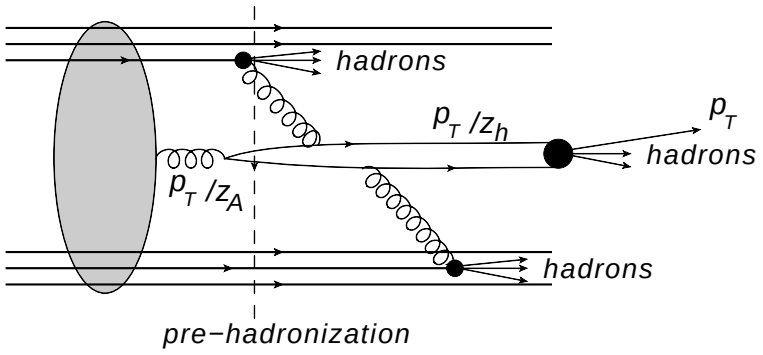

FIG. 2: Inclusive production of hadrons in nucleus-nucleus collision through the stage of pre-hadronization.

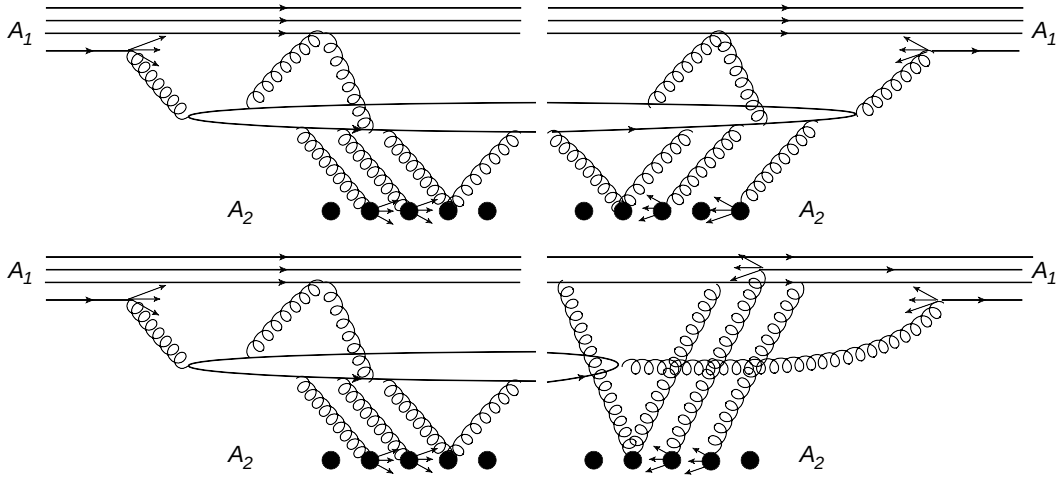

FIG. 3: Inclusive production of quark-antiquark pair (dipole) in nucleus-nucleus collisions.

interactions occur with other nucleons in both nuclei in the amplitude. In the complex conjugate amplitude the same happens with a dipole with a transverse size r'. Note that for simplicity we assumed that the nuclear profile is cylindrical $T(b) \approx 2R_A$ with $b^2 \leq R_A^2$.

The dipole-nucleon cross-section can be written as

$$\sigma\left(Y,r\right) \,=\, \frac{4\pi^2\alpha_s}{N_c}\int \frac{d^2l}{2\pi l^2}\,\left(1-e^{i\,\underline{r}\cdot\underline{l}}\right)\,\left(1-e^{-i\,\underline{r}\cdot\underline{l}}\right)\,\phi\left(Y,l^2\right)\,\xrightarrow{\underline{r}\cdot\underline{l}\ll 1}\,\frac{2\pi^2\alpha_s}{N_c}\,r^2\int dl^2\phi\left(Y,l^2\right), \tag{6}$$

where ϕ is the unintegrated gluon density, Y is the rapidity of the dipole. In the right side of the above equation we have kept only the dominant contribution relevant at large transverse momentum of the produced dipole in the DGLAP approximation. Using Eq. (6), one can simplify Eq. (5) by the following replacement [33, 55]:

$$\sigma\left(Y,r\right)\,\rho\,T(b) \approx \sigma\left(Y,r^2\right)\,\rho\,2R_A\,\rightarrow r^2Q_{si}^2/8, \tag{7}$$

where Q_{si} is the gluon saturation momentum in the nuclei i and can also depend on the impact-parameter b. In the same fashion, for inelastic dipole-nucleon cross-section we have the following expression

$$\begin{aligned}\sigma_{in}\left(Y,r,r'\right) \,&=\, 2\,\frac{4\pi^2\alpha_s}{N_c}\int \frac{d^2l}{2\pi l^2}\,\left(1-e^{i\,\underline{r}\cdot\underline{l}}\right)\left(1-e^{-i\,\underline{r'}\cdot\underline{l}}\right)\,\phi\left(Y,l^2\right)\,\xrightarrow{\underline{r}\cdot\underline{l}\ll 1}\,\frac{2\pi^2\alpha_s}{N_c}\,2\,\underline{r}\cdot\underline{r'}\int dl^2\phi\left(Y,l^2\right),\\ \sigma_{in}\left(Y,r,r'\right)\,\rho\,2R_A \,&\rightarrow\, 2\underline{r}\cdot\underline{r'}Q_{si}^2/8.\end{aligned} \tag{8}$$

Note that Eq. (4) integrated over the impact-parameter b gives the inclusive cross-section for $q\bar{q}$-pair with a relative transverse momentum k. It incorporates the first stage of the process, namely the parton production (shown as a dark blob in Fig. 2). Here, we assumed that the produced quark-antiquark pair is moving in the classical gluon field, neglecting the evolution in the rapidity interval y. We believe that this assumption will not be essential in estimating the energy loss.

In calculating the average energy loss, we assume that in each inelastic interaction, the dipole energy decreases z_h times due to the pre-hadronization process. For elastic interaction we also introduce factor $z_{h,el}$ which describes the fraction of energy that is carried by the fastest hadron. For simplicity we assume that $z_h = z_{h,el}$. For elastic scattering the energy loss emerges only on the last stage, namely quark-antiquark (or gluon) hadron transition. An additional source of the energy loss in nucleus collisions stems from the inelastic interaction of $q\bar{q}$-pairs (or gluons). In this process, soft gluons (slower than propagating $q\bar{q}$-pair or gluon) are produced. Then, these gluons produce hadrons due to hadronization and these hadrons carry $(1 - z_h)$ energy of colliding gluon. Due to this process, the propagating gluon loses z_h fraction of energy per each inelastic interaction. In order to calculate the resulting average energy-loss of the dipole propagating through the medium, in Eqs. (4,5) one needs to multiply every σ_{in} by the factor z_h. From Eqs. (6,8) one can see that each factor $\underline{r} \cdot \underline{r'}$ is associated with the inelastic interaction. Therefore, this multiplication can be carried out by the following replacement in Eq. (4),

$$(\underline{r} - \underline{r'})^2 \;=\; r^2 + r'^2 - 2\underline{r} \cdot \underline{r'} \;\to\; r^2 + r'^2 - 2\, z_h\, \underline{r} \cdot \underline{r'}. \tag{9}$$

The average energy loss can be then obtained from the following expression

$$\langle z_h \rangle_A \;\equiv\; z_A \;=\; \Big((z_h \,-\, 1)\; P^{q\bar{q}}_{AA}\,(y, b, k; z_h = 0) \;+ P^{q\bar{q}}_{AA}\,(y, b, k; z_h) \Big) \Big/ P^{q\bar{q}}_{AA}\,(y, b, k; z_h = 1)\,. \tag{10}$$

In the above equation, the first term only takes into account the processes of hadronization of the quark-antiquark with rapidity y that passes through the medium without an inelastic interaction. The second term in Eq. (10) is responsible for hadrons production in the entire kinematic region of rapidity y. Note that Eq. (10) is based on the assumption that if no energy-loss occurs in a single interaction $z_h = 1$ then no energy-loss will follow in multiple-interactions namely $z_A = 1$, and if the parton loses all its energy in a single interaction $z_h = 0$ then naturally in multiple-interactions we have also $z_A = 0$. The NMF Eq. (3) incorporating the pre-hadronization energy-loss effect, can be then rewritten in the following form,

$$\text{NMF} \;=\; \frac{1}{A^2}\,\frac{S^2_A}{S^2_p}\,\frac{\mathcal{T}\Big(p_T \Big/ (z_A\, Q_{s,A})\Big)}{\mathcal{T}\Big(p_T \Big/ (z_h\, Q_{s,N})\Big)}. \tag{11}$$

In Eq. (11) we use the fact that the transverse momentum of the emitted gluon in pp or AA collisions is equal to [27],

$$p^2_T\,(\text{gluon}) \;=\; p^2_T\,(\text{hadron})\,/z^2_{h,A} \;+\; k^2_T\,(\text{intrinsic})\,, \tag{12}$$

where k_T (intrinsic) is the average intrinsic transverse momentum of the gluonic jet and since its value is small, it can be neglected.

B. Gluon pre-hadronization model

In the second model, we consider a case that the produced gluon decays into hadrons after propagating through the nucleus (see Fig. 4).

Using the approaches suggested in Refs. [17, 58, 59] and summing all gluon exchange diagrams shown in Fig. 5 and neglecting again the small-x evolution in the rapidity interval between the produced gluon and the target, the probability of gluon production in AA collisions with a transverse momentum k can be written in the following form,

$$\begin{aligned} P^G_{AA}\,(y, b, k) \;=\; & \frac{\alpha_s\, Q^2_{s1}}{8\pi^4} \int d^2r \int d^2r'\, e^{-i\frac{1}{2}\underline{k}\cdot(\underline{r}-\underline{r'})} \Big\{ K_2\,(kr)\; K_2\,(kr')\; J_0\,(kr)\; J_0\,(kr') \Big\} \\ \times \; & \frac{8\, C_F}{\pi^2 \alpha_s} \Big\{ \frac{1}{r^2} \Big(1 - e^{-\frac{1}{4}\underline{r}^2 Q^2_{s1}}\Big) \Big(1 - e^{-\frac{1}{4}\underline{r}^2 Q^2_{s2}}\Big) + \frac{1}{r'^2} \Big(1 - e^{-\frac{1}{4}\underline{r'}^2 Q^2_{s1}}\Big) \Big(1 - e^{-\frac{1}{4}\underline{r'}^2 Q^2_{s2}}\Big) \\ & - \; \frac{1}{(\underline{r} - \underline{r'})^2} \Big(1 - e^{-\frac{1}{4}(\underline{r}-\underline{r'})^2 Q^2_{s1}}\Big) \Big(1 - e^{-\frac{1}{4}(\underline{r}-\underline{r'})^2 Q^2_{s2}}\Big) \Big\}. \end{aligned} \tag{13}$$

In the derivation of the above equation, we assume that the gluon with transverse momentum k is emitted by the dipole with transverse size smaller than $1/k$. Indeed, all rescattering of the gluons emitted by dipoles with larger sizes are already included in Eq. (2) [17]. In this case the emission of gluon from interaction with a nucleon can be considered as a decay of the nucleon to two colorless dipoles. This can be better conceived at large N_c limit where

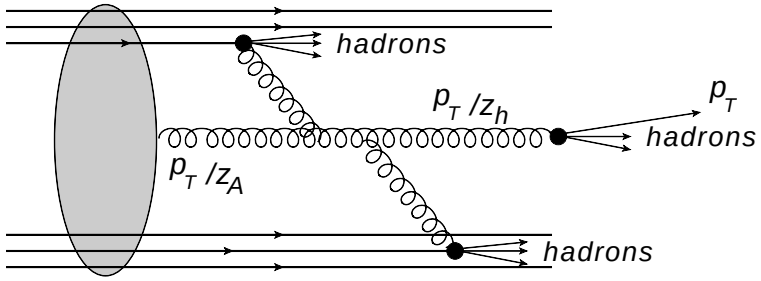

FIG. 4: Inclusive production of hadrons in nucleus-nucleus collision due to gluon decay.

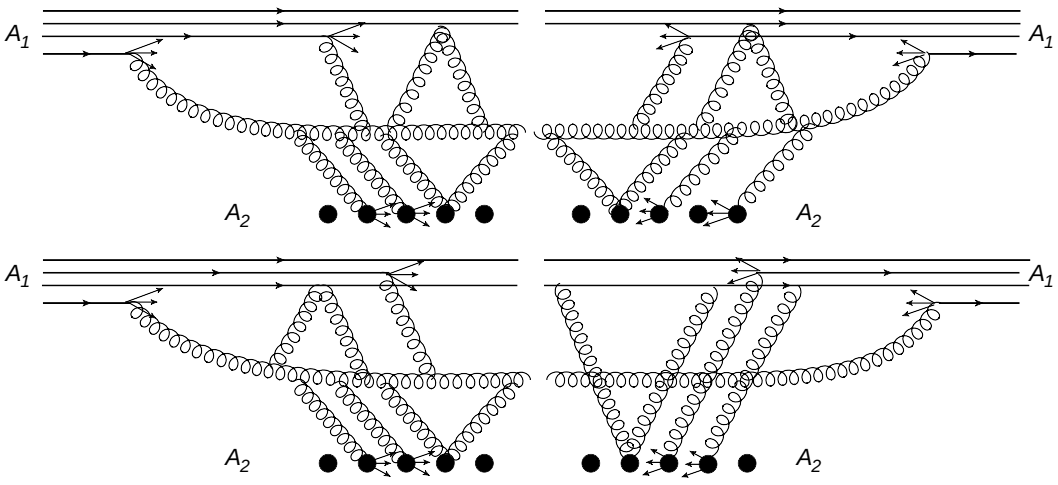

FIG. 5: The passage of the produced gluon in nucleus-nucleus collision.

an adjoint (gluon) dipole can be decomposed into two fundamental (quark) dipoles. These two dipoles penetrate through the medium with the same cross section. The wave function of such a gluon has been calculated in Ref. [61]. Therefore, this approach differs from the quark-antiquark pre-hadronization model mainly by the value of the dipole cross section: $\sigma_G\left(Y, r^2\right) \approx 2\sigma_{dipole}$. In other words, the main differences between Eq. (13) and Eq. (4) is that in Eq. (13) the value of the saturation momentum is two times larger than in Eq. (4).

In order to calculate the average energy loss of the produced gluon at the pre-hadronization stage $\langle z_h \rangle_A$, we again follow the steps in Eqs. (9,10) by replacing $P_{AA}^{q\bar{q}} \to P_{AA}^{G}$. The corresponding NMF can be then obtained by Eq. (11).

It is worthwhile mentioning that in Eq. (11) we take into account both the first stage, namely $q\bar{q}$-pair (or gluon) production (the dark blobs in Figs. 2, 4), and also the energy-loss effect due to the passage of the produced $q\bar{q}$-pair (or gluon) through the medium (see Figs. 3, 5). In a sense, we unfolded the k_T factorization and made the corresponding corrections due to the pre-hadronization energy-loss effect since the hadronization leads to its violation.

III. LARGE p_T BEHAVIOR OF NMF

At very large p_T, the pQCD factorization theorem [7–11] can be used. The production of gluon-jet with transverse momentum p_T (see Fig. 6) in nucleus-nucleus collisions can be simply written as

$$\begin{aligned} \frac{d\sigma_{AA}}{dy, d^2p_T}|_{y=0} &= A^2 \frac{d\sigma_{pp}}{dy, d^2p_T} = \sigma_{\rm hard}\, x_1 G_A\left(x_1 = 2p_T/\sqrt{s}, p_T\right)\, x_2 G_A\left(x_2 = 2p_T/\sqrt{s}, -p_T\right), \qquad (14) \\ &= A^2 \frac{\alpha_s^2(p_T)}{p_T^4}\, x_1 G_p\left(x_1 = 2p_T/\sqrt{s}, p_T\right)\, x_2 G_p\left(x_2 = 2p_T/\sqrt{s}, -p_T\right) \to A^2 \frac{\alpha_s^2(p_T)}{p_T^4}\left(p_T^2/Q_0^2\right)^{2\gamma}, \end{aligned}$$

where xG_P (or xG_A) is the gluon structure function for the proton (or nucleus) and Q_0 is a separation scale so as for $p_T > Q_0$ one can use perturbative QCD. In the above expression, $\sigma_{\rm hard}$ is the perturbative partonic cross section computable up to a given order in α_s, and γ denotes the anomalous dimension. It is well-known that in the

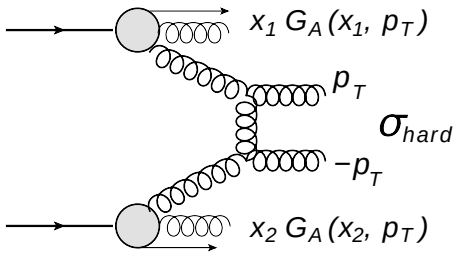

FIG. 6: The gluon production accordingly to the factorization theorem at large p_T.

leading-order for $x \to 1$ we have $\gamma \to \alpha_s$. Therefore, at very large $p_T \gg Q_s$ but $p_T \ll \sqrt{s}$, the NMF obtained via Eqs. (1,12,14) is equal to

$$\text{NMF} \xrightarrow{\sqrt{s} \gg p_T \gg Q_s} \frac{\alpha_s^2\left(p_T/z_A\right)\left(p_T/z_A\right)^{4\alpha_s(p_T/z_A)}}{\alpha_s^2\left(p_T/z_h\right)\left(p_T/z_h\right)^{4\alpha_s(p_T/z_h)}} \times \left(\frac{z_A}{z_h}\right)^4. \tag{15}$$

The value of the NMF can be then immediately estimated at large p_T via Eq. (15) by only knowing the value of z_A, z_h and also Λ_{QCD} which appears in the running strong-coupling. For the running coupling α_s, we employ the scheme used in Ref. [27] at the leading-order. We postpone the numerical discussion to the next section, and in the rest of this section, we address another important question, namely at which p_T the expression given in Eq. (15) can be used. Let us for sake of simplicity work in double log approximation with the anomalous dimension $\gamma = \bar{\alpha}_s/\omega$ where ω is Mellin image of $\ln(1/x)$ and $\bar{\alpha}_s = \alpha_s N_c/\pi$. In such an approximation, the nuclear gluon structure function up to a numerical constant $\mathcal{K}$ can be written as [62]

$$\begin{aligned}\frac{xG_A\left(x = 2p_T/\sqrt{s}, p_T\right)}{p_T^2} &= \mathcal{K}\,\exp\left(\sqrt{4\bar{\alpha}_s \ln(1/x)\,\ln\left(p_T^2/Q_0^2\right)} \;-\; \ln\left(p_T^2/Q_0^2\right) \;+\; l_A\right)\,, \\ &= \mathcal{K}\,\exp\left(\sqrt{L\,\ln\left(p_T^2/Q_0^2\right)} \;-\; \ln\left(p_T^2/Q_0^2\right) \;+\; l_A\right), \end{aligned} \tag{16}$$

where $L = 4\bar{\alpha}_s \ln(1/x) = \ln\left(Q_s^2\left(A;x\right)/Q_s^2\left(A;x=x_0\right)\right)$ and $l_A = (1/3)\ln A$. The equation for the saturation scale has the form [62],

$$L\, l_s \;=\; (l_s - l_A)^2, \tag{17}$$

with a solution,

$$l_s\left(L, l_A\right) \equiv \ln\left(Q_s^2\left(A;x\right)/Q_0^2\right) \;=\; \frac{L}{2} \;+\; l_A\,\sqrt{\left(\frac{L}{2}\right)^2 \;+\; L\, l_A}. \tag{18}$$

One can see that G_A given by Eq. (16) at $Q^2 = Q_0^2$ is proportional to $A^{1/3}$. Introducing a new variable $\mathcal{Z} = \ln\left(p_T^2/Q_s^2\left(A;x\right)\right)$ one can rewrite Eq. (16) in the following form

$$\frac{xG_A\left(x = 2p_T/\sqrt{s}, p_T\right)}{p_T^2} \;=\; \mathcal{K}\,\exp\left(H\left(\mathcal{Z}, L, l_A\right)\right), \tag{19}$$

with a notation,

$$H\left(\mathcal{Z}, L, l_A\right) \;=\; \sqrt{L\left(\mathcal{Z} + l_s\left(L, l_A\right)\right)} \;-\; \mathcal{Z} \;-\; l_s\left(L, l_A\right) \;+\; l_A. \tag{20}$$

Expanding $H\left(z, L, l_A\right)$ at small z, we have

$$H\left(\mathcal{Z}, L, l_A\right) \;=\; -\,h_1\left(L, l_A\right)\,\mathcal{Z} \;+\; h_2\left(L, l_A\right)\,\mathcal{Z}^2 \;+\; \mathcal{O}\left(\mathcal{Z}^3\right), \tag{21}$$

with

$$h_1\left(L, l_A\right) \;=\; 1 \;-\; \frac{L}{2\sqrt{\frac{L^2}{2} \;+\; L\, l_A \;+\; L\,\sqrt{l_A^2 \;+\; \left(\frac{L}{2} + l_A\right)^2}}}, \tag{22}$$

$$h_2\left(L, l_A\right) \;=\; \frac{L^2}{2\sqrt{2}\left(L\left(L + 2l_A + \sqrt{L^2 + 4Ll_A + 8l_A^2}\right)\right)^{3/2}}. \tag{23}$$

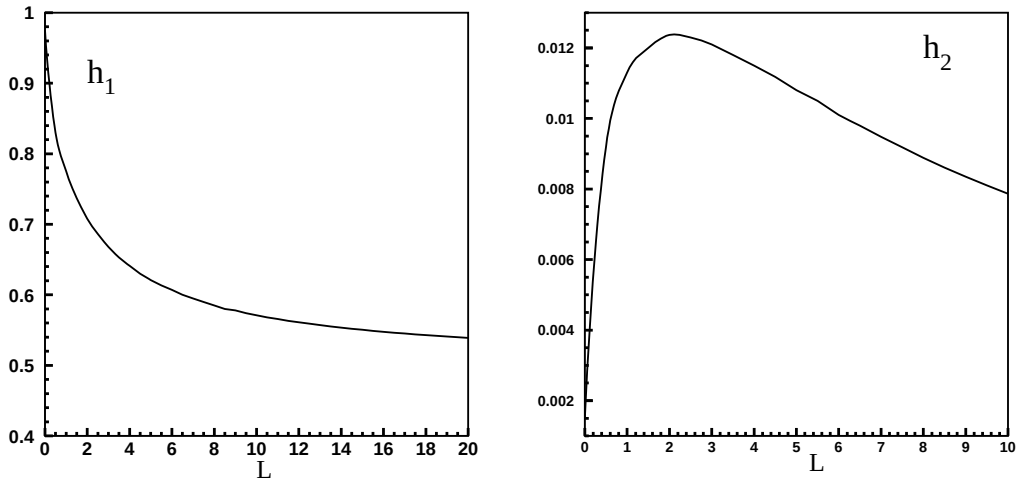

FIG. 7: Function h_1 and h_2 defined in Eqs. (22,23) versus L.

The function h_1 and h_2 versus L for the gold are shown in Fig. 7. It is seen that at large values of L, we have $h_1 \to 1/2$ and $h_2 \to 1/8L$ in accordance with finding in Ref. [30]. Using the KLN saturation model parametrization, the value of L is about $L \approx 1$ and 1.7 for RHIC and the LHC energies, respectively [31]. The condition [30]

$$h_2\, \mathcal{Z}^2 \,>\, 1, \tag{24}$$

characterizes that $\mathcal{Z}$ is large and the scattering amplitude is far away from the saturation domain, out of the region where we have the geometric scaling behavior at large values of L. Indeed, the first term in Eq. (21) leads to the geometric scaling behavior at large values of L while the second term violates this behavior even at large L. Therefore, the condition given in Eq. (24) ensures that the gluon structure function defined in Eq. (19) gives the perturbative form used in Eq. (14).

Eq. (24) leads to $p_T > 40$ GeV for the RHIC energies and to $p_T > 60$ GeV for the LHC energies for the produced gluon. In terms of the transverse momenta of the produced hadron we expect that for $p_T \geq 40\, z_A \approx 15$ GeV at the RHIC and for $p_T \geq 60\, z_A \approx 25$ GeV at the LHC, the NMF defined in Eq. (15) to be reliable. Notice that if the pre-hadronization stage in AA and pp collisions was the same, namely $z_A = z_h$, then the NMF defined in Eq. (15) was identically equal to one $R_{AA} = 1$. Therefore, the main source of suppression of the NMF for hadrons at high-p_T is due to further energy loss of the produced gluons in AA collisions compared to pp collisions at the pre-hadronization stage, namely $z_A < z_p$. Notice that on average z_A and z_p vary slowly with p_T for the kinematic region of our interest here [28]. Note also that the p_T-dependence in Eq. (15) mainly enters through the running of the strong-coupling. This justify the flatness of the NMF R_{AA} over large range of p_T. In the next section we show that the numerical value obtained for z_A from the pre-hadronization mechanisms introduced in section II can indeed describe the observed suppression of hadrons at large-p_T at RHIC. For smaller values of p_T, Eq. (2) may be used with the dipole amplitude N being in the region where we still have the geometric scaling behavior for $N \equiv N(z)$ [30].

IV. NUMERICAL RESULTS AND COMPARISON WITH EXPERIMENTAL DATA

In order to estimate the value of $\langle z_h \rangle_A$, we use the KLN saturation parametrization [31] with $Q_s = 1.41$ GeV at $\sqrt{s} = 200$ GeV for gold and we take $k = 2$ GeV as a typical scale for soft interaction. The chosen soft interaction scale corresponds to the value of the soft Pomeron slope $k \approx 1/\sqrt{\alpha'_{I\!P}}$ with $\alpha'_{I\!P} = 0.25\,\text{GeV}^{-2}$ [59, 60, 63]. It turns out that both pre-hadronization models give very close values for $\langle z_h \rangle_A / z_h$: 0.766 and 0.744 for the quark-antiquark and the gluon pre-hadronization model respectively, at the RHIC energy $\sqrt{s} = 200$ GeV. The value of $z_h \approx 1/2$ was obtained from a fit to the experimental data in pp collisions for the average transverse momentum of charged hadrons for a wide range of energies [27].

Again using the KLN parametrization for the nuclear saturation scale, we estimated the value of $\langle z_h \rangle_A / z_h$ at the LHC energies, assuming $z_h \approx 1/2$. At higher energies or larger value of the saturation scale Q_s, one can approximate the integrand of Eqs. (4,13) to its maximum value at $r = r\prime \approx 1/Q_s$. This leads to a similar value for z_A in both

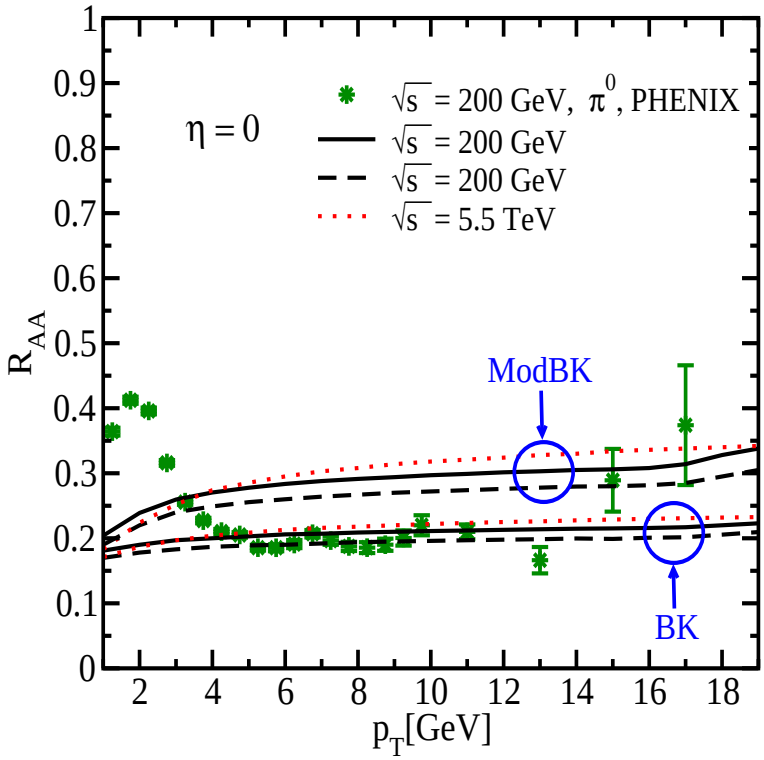

FIG. 8: The NMF for hadrons obtained by Eq. (11) for $0-10\%$ centrality $Au+Au$ collisions at various energies. Function $\mathcal{T}(x_\perp)$ is calculated using the solution of the BK and the modified BK equations. The solid and dashed lines correspond to the quark-antiquark and gluon pre-hadronization models, respectively. The experimental data is taken from Ref. [1].

pre-hadronization models at higher energies, since the over-all factors in Eqs. (4,13) will be canceled out via Eq. (10). Indeed, full numerical solution is in accordance with this observation and we found that both pre-hadronization models result to a very similar value for z_A at the LHC energies, namely $\langle z_h\rangle_A/z_h \approx 0.82,\ 0.795$ at $\sqrt{s} = 5.5,\ 2.75$ TeV, respectively.

Our results for the NMF for $0-10\%$ centrality in $Au+Au$ collisions using the k_t factorization Eq. (11) supplemented with solutions of the BK and the modified BK equation that preserves the energy conservation [64] is shown in Fig. 8. In the modified BK equation (denoted by ModBK in Fig. 8), the next-to-leading order corrections to the BFKL kernel are taken into account which leads to conservation of energy in the framework of non-linear equation [65]. We recall that here we resort to the LPHD principle for the final state hadronization. But the energy-loss effect in the pre-hadronization both in pp and AA collisions are effectively incorporated in the results shown in Fig. 8. We believe that the difference between two pre-hadronization models (introduced in Sec. II) in AA collisions gives reasonable estimates of the errors which are unavoidable in the situation that we do not know the theory of pre-hadronization in a dense medium. As we already pointed out, the differences between these two pre-hadronization models at LHC is negligible. The energy-loss effect reduces the NMF defined in Eq. (11) about $30 \div 50\%$. Notice that this reduction does not depend on a given BK solution and incorporates the missing energy-loss effect into the k_T factorization.

We should stress that the numerical estimates in Fig. 8 was obtained from the BK equation with a simplified kernel [62, 64]. Such estimates is less reliable for describing the experimental data, even though, interesting enough, such a rough approximation apparently is in agreement with RHIC data at high-p_T within the errors. Notice that in fact the validity of the k_T factorization Eq. (11) beyond the extended geometric-scaling region at high-p_T is questionable, see also Sec. I. An important message here is that the smallness and the high-p_T flatness of the NMF obtained from Eq. (11) and the BK equation is rather generic and it does not strongly depend on the details of the BK solutions in our interested kinematic region here, see also recent interesting paper by Albacete and Marquet [66]. It is also seen from Fig. 8 that as one may expect, the onset of the flatness of the NMF at the LHC energy occurs at higher p_T. Fig. 8 indicates that the energy-conservation constrain on the BK equation which is important at higher p_T tends to enhance the NMF. This is due to the fact that the ModBK solution correctly incorporates the behavior of the anomalous dimension at large Bjorken-x by matching to the DGLAP value.

In order to make more reliable prediction for the NMF for the neutral pion π^0, we next re-calculate the NMF from Eq. (11) by using the impact-parameter dependent CGC saturation model in pp [27] and AA collision [28]. It

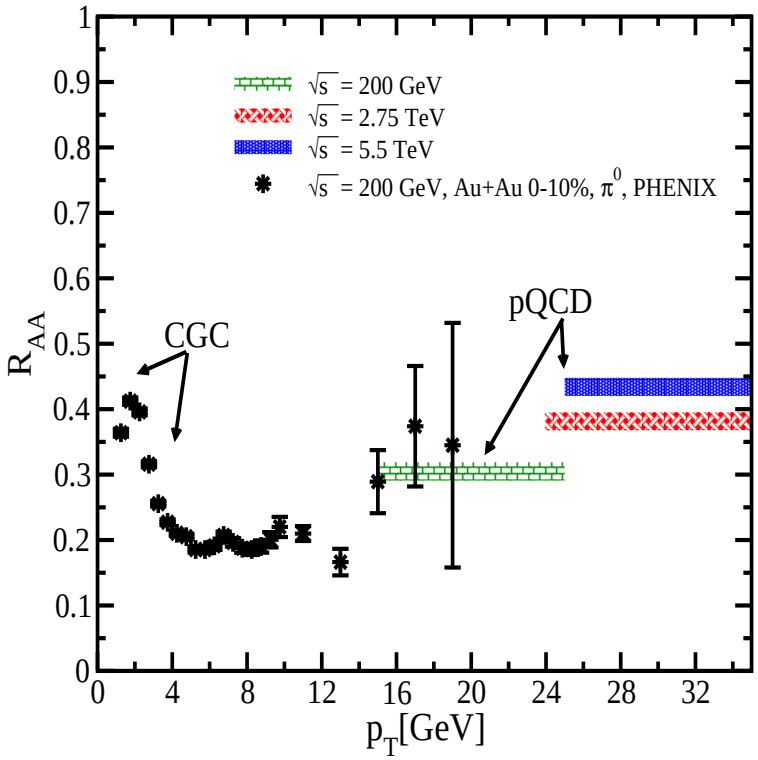

FIG. 9: The NMF for hadrons obtained by Eq. (11) at low p_T and Eq. (15) at high p_T for $0-10\%$ centrality AA collisions at various energies. Function $\mathcal{T}(x_\perp)$ is calculated within the CGC approach [27, 28]. The experimental data is taken from Ref. [1].

has been already shown that such a scheme describes HERA data at small-x [67] and the hadron multiplicities in nucleus-nucleus collisions at RHIC [28] and provided correct predictions [27] for the inclusive hadron production at the LHC. The importance of the inclusion of the impact-parameter dependence in the saturation models and the BK equation has been addressed in Refs. [27, 28, 68]. Our results at RHIC and the LHC energies in $0-10\%$ centrality $Au+Au$ (at RHIC) and $Pb+Pb$ (at the LHC) collisions, is shown in Fig. 9. We recall that Eq. (11) has $x_\perp$-scaling property which is valid only at low transverse momentum roughly for $p \leq 3 \div 4Q_S$. In the saturation model [67] used in Fig. 9, the saturation scale varies very slowly with energy and for $p_T = 1$ GeV at midrapidity for central collisions we have $Q_s = 0.76$ GeV for proton at $\sqrt{s} = 5.5$ TeV. Therefore, the upper limit of $x_\perp$-scaling behavior in this model is about $p_T \approx 3$ GeV for pp collisions (the reference for the NMF) at $\sqrt{s} = 5.5$ TeV at midrapidity. We therefore, only show the CGC results coming from Eq. (11) for $p_T < 4$ GeV. Here, we only concentrate on the CGC results at rather low-p_T where we can also give a good description of spectra in pp collisions [27]. At the RHIC energy $\sqrt{s} = 200$ GeV at mid-rapidity, for $p_T > 2$ GeV, we have $x > 0.01$ which is beyond the validity of the CGC prescription. Note also that the dipole model used here was obtained from a fit to HERA data for virtuality $Q^2 \in [0.25, 45]$ GeV^2. Therefore, this model is valid for $p_T \in [0.7, 6.7]$ GeV. Again, we employ the LPHD principle to connect pre-hadronization to final hadronization stage. This leads to two different over-all factors for the spectra in pp and AA collisions which are fixed with the experimental data at lower energies [27, 28]. The appearance of two different over-all factors for the normalization is partly due to the fact that pre-hadronization leads to different effective masses for the mini-jet in AA and pp collisions [27, 28]. It is seen from Fig. 9 that our results without any free-parameter to adjust, is in accordance with the PHENIX data at low-p_T, in contrast to the impact-parameter independent BK solution shown in Fig. 9 with a zero mini-jet mass. At low-p_T, the energy-loss in medium is less important and we have taken $z_A = z_h = 1/2$ for $p_T < 4$ GeV.

At high-p_T, we rely on the improved pQCD factorization result given in Eq. (15) (also shown in Fig. 9). The only external parameter in the NMF defined in Eq. (15) is the parameter z_A which incorporates the energy-loss effect at the pre-hadronization stage. The value of the parameter z_A was already calculated in Sec. II (see also above) at RHIC and the LHC energies. As we already argued Eq. (15) is valid at high transverse momentum of the produced hadrons for $p_T \geq 40\, z_A \approx 15$ GeV at RHIC and for $p_T \geq 60\, z_A \approx 25$ GeV at the LHC energies. Our predictions for the NMF suppression and the onset of the flatness of the NMF at high-p_T both agree with the PHENIX data. As we already pointed out Eq. (15) naturally leads to the flatness of the NMF at high p_T since p_T dependence mainly

enters via the running strong-coupling and varies very slowly with p_T. In Fig. 9, we also show our predictions both at low and high p_T at the LHC energies $\sqrt{s} = 2.75$ and 5.5 TeV. The uncertainties in our formulation is less than 10% which come mainly from the normalization in Eq. (11). The band in Fig. 9 indicates about 2% theoretical error which also includes the discrepancies between two pre-hadronization schemes. The predictions of other approaches at the LHC can be found in Ref. [69].

V. CONCLUSIONS

In this paper first we developed a simple picture for calculating the energy-loss effect. In our approach, the energy-loss effect stems from the process of the pre-hadronization. We showed that the estimates of the energy-loss in two different models of the pre-hadronization lead to very close values and is able to explain the measured R_{AA} at high transverse momentum of produced hadrons at RHIC. We showed that the small value of the nuclear modification factor at high-p_T is mainly due to the energy-loss effect in the pre-hadronization stage.

We also investigated the NMF obtained from the k_T factorization supplemented with solutions of the BK and the modified BK equation that preserves the energy conservation. We showed that the smallness ($R_{AA} < 0.5$) and the high-p_T flatness of the NMF obtained from Eq. (11) and the BK equation is rather generic and it does not strongly depend on the details of the BK solutions. We showed that the modified BK solution which includes the energy conservation tends to slightly enhance the NMF at high-p_T. This is due to the fact that the modified BK equation properly includes the anomalous dimension at $x \approx 1$ which coincides with the anomalous dimension of the DGLAP equation while the BK equation only reproduces its double log limit. This indicates that one should be cautious as extrapolating the k_T factorization results to higher p_T is less reliable if the running anomalous dimension obtained from the BK solution does not match to the DGLAP value at high-p_T.

We showed that at high-p_T, the pQCD factorization incorporated with the pre-haronization energy-loss effect Eq. (15) results naturally to flatness of the NMF. We obtained the onset of the applicability of Eq. (15) to be for $p_T > 40$ GeV at RHIC and for $p_T > 60$ GeV at the LHC for the produced gluon. Notice that in this kinematic region the NMF for the produced jet should approach to one $R^g_{AA} \to 1$. However, the NMF of the produced hadron is very small $R^{\pi^0}_{AA} < 0.5$ due to the pre-hadronization effect, namely $z_A/z_p < 1$. In terms of the transverse momenta of the produced hadron we expect that this to be for $p_T \geq 15$ GeV at RHIC and for $p_T \geq 25$ GeV at the LHC.

Acknowledgments

This work was supported in part by Conicyt Programa Bicentenario PSD-91-2006 and the Fondecyt (Chile) grants 1090312 and 1100648.

[1] A. Adare *et al.* [PHENIX Collaboration], Phys. Rev. **C82** (2010) 011902 [arXiv:1005.4916].
[2] I. Arsene *et al.* [BRAHMS Collaboration], Phys. Rev. Lett. **91** (2003) 07305.
[3] I. Arsene *et al.* [BRAHMS Collaboration], Phys. Rev. Lett. **93** (2004) 242303 [nucl-ex/0403005].
[4] I. Arsene *et al.* [BRAHMS Collaboration], Phys. Lett. **B650** (2007) 219 [nucl-ex/0610021].
[5] S. S. Adler *et al.* [PHENIX Collaboration], Phys. Rev. Lett. **96** (2006) 032301 [nucl-ex/05100].
[6] M. J. Tannenbaum, *"Critical examination of RHIC paradigms-mostly high pT "*, Workshop on Critical Examination of RHIC Paradigms, Austin, TX, April 14-17 (2010), arXiv:1008.1536.
[7] J. C. Collins, D. E. Soper and G. F. Sterman, Adv. Ser. Direct. High Energy Phys. **5** (1988) 1 [hep-ph/0409313].
[8] J. C. Collins, D. E. Soper and G. F. Sterman, Nucl. Phys. **B308** (1988) 833.
[9] G. T. Bodwin, Phys. Rev. **D31** (1985) 2616; Phys. Rev. **D34** (1986) 3932.
[10] J. C. Collins, D. E. Soper and G. F. Sterman, Nucl. Phys. **B261** (1985) 104.
[11] X-N. Wang, Phys. Rev. **C61** (2000) 064910; for a review see: J. F. Owens, Rev. Mod. Phys. **59** (1987) 465.
[12] L. V. Gribov, E. M. Levin and M. G. Ryskin, Phys. Rep. **100** (1983) 1.
[13] A. H. Mueller and J. Qiu, Nucl.Phys. **B268** (1986) 427; J.-P. Blaizot and A. H. Mueller, Nucl. Phys. **B289** (1987) 847.
[14] L. McLerran and R. Venugopalan, Phys. Rev. **D49** (1994) 2233; **D49** (1994) 3352; **D50**, (1994) 2225; **D53** (1996) 458; **D59** (1999) 094002.
[15] I. Balitsky, Nucl. Phys. **B463** (1996) 99; Y. Kovchegov, Phys. Rev. **D60** (2000) 034008.
[16] J. Jalilian-Marian, A. Kovner, A. Leonidov and H. Weigert, Phys. Rev. **D59** (1998) 014014 [hep-ph/9706377]; Nucl. Phys. **B504** (1997) 415 [hep-ph/9701284]; E. Iancu, A. Leonidov and L. D. McLerran, Phys. Lett. **B510** (2001) 133 [hep-ph/0102009]; Nucl. Phys. **A692** (2001) 583 [hep-ph/0011241]; H. Weigert, Nucl. Phys. **A703** (2002) 823 [hep-ph/0004044].

[17] Y. V. Kovchegov and K. Tuchin, Phys. Rev. **D65** (2002) 074026 [hep-ph/0111362].
[18] M. A. Braun, Eur. Phys. J. **C48** (2006) 501 [hep-ph/0603060].
[19] M. A. Braun, Phys. Lett. **B483** (2000) 105 [hep-ph/0003003].
[20] C. Marquet, Nucl. Phys. **B705** (2005) 319 [hep-ph/0409023].
[21] A. Kovner and M. Lublinsky, JHEP **0611** (2006) 083 [hep-ph/0609227].
[22] E. Levin and A. Prygarin, Phys. Rev. **C78** (2008) 065202 [arXiv:0804.4747].
[23] S. Catani, M. Ciafaloni and F. Hautmann, Nucl. Phys. **B366** (1991) 135.
[24] S. Catani, M. Ciafaloni and F. Hautmann, Nucl. Phys. Proc. Suppl. **A29** (1992) 182.
[25] J. C. Collins and R. K. Ellis, Nucl. Phys. **B360** (1991) 3.
[26] E. M. Levin, M. G. Ryskin, Yu. M. Shabelski and A. G. Shuvaev, Sov. J. Nucl. Phys. **53** (1991) 657 [Yad. Fiz. **53** (1991) 1059].
[27] E. Levin and A. H. Rezaeian, Phys. Rev. **D82** (2010) 014022 [arXiv:1005.0631].
[28] E. Levin and A. H. Rezaeian, Phys. Rev. **D82** (2010) 054003 [arXiv:1007.2430].
[29] J. Bartels and E. Levin, Nucl. Phys. **B387** (1992) 617; A. M. Stasto, K. J. Golec-Biernat, and J. Kwiecinski, Phys. Rev. Lett. **86** (2001) 596.
[30] E. Iancu, K. Itakura and L. McLerran, Nucl. Phys. **A708** (2002) 327 [hep-ph/0203137].
[31] D. Kharzeev and M. Nardi, Phys. Lett. **B507** (2001) 121; D. Kharzeev and E. Levin, Phys. Lett. **B523** (2001) 79; D. Kharzeev, E. Levin and M. Nardi, Phys. Rev. **C71** (2005) 054903; D. Kharzeev, E. Levin and L. McLerran, Phys. Lett. **B561** (2003) 93.
[32] B. Z. Kopeliovich, A. H. Rezaeian, H. J. Pirner and I. Schmidt, Phys. Lett. **B653** (2007) 210 [arXiv:0704.0642]; arXiv:0707.2040; B. Z. Kopeliovich, H. J. Pirner, A.H. Rezaeian and I. Schmidt, Phys. Rev. **D77** (2008) 034011 [arXiv:0711.3010]; B. Z. Kopeliovich, A. H. Rezaeian and I. Schmidt, Nucl. Phys. **A807** (2008) 61 [arXiv:0712.2829]; B. Z. Kopeliovich, E. Levin, A. H. Rezaeian and I. Schmidt, Phys. Lett. **B675** (2009) 190 [arXiv:0902.4287].
[33] A. H. Rezaeian and A. Schäfer, Phys. Rev. **D81** (2010) 114032 [arXiv:0908.3695].
[34] S. Turbide, C. Gale, E. Frodermann and U. Heinz, Phys. Rev. **C77** (2008) 024909.
[35] A. H. Mueller, Phys. Lett. **B668** (2008) 11 [arXiv:0805.3140].
[36] B. Z. Kopeliovich, arXiv:1007.4513.
[37] A. Adare *et al.* [PHENIX Collaboration], Phys. Rev. Lett. **98** (2007) 232301 [nucl-ex/0611020].
[38] A. Adare *et al.* [PHENIX Collaboration], Phys. Rev. Lett. **101** (2008) 122301 [arXiv:0801.0220].
[39] B. I. Abelev *et al.* [STAR Collaboration], Phys. Rev. **C80** (2009) 041902 [arXiv:0904.0439].
[40] R. Baier, A. H. Mueller, D. T. Son and D. Schiff, Nucl. Phys. **A698** (2002) 217; R. Baier, Y. L. Dokshitzer, A. H. Mueller and D. Schiff, JHEP **0109** (2001) 033 [hep-ph/0106347]; Phys. Rev. **C60** (1999) 064902 [hep-ph/9907267]; Nucl. Phys. **B531** (1998) 403 [hep-ph/9804212]; Nucl. Phys. **B484** (1997) 265 [hep-ph/9608322]; Nucl. Phys. **B483** (1997) 291 [hep-ph/9607355].
[41] B. G. Zakharov, JETP Lett. **63** (1996) 952 [hep-ph/9607440].
[42] B. G. Zakharov, JETP Lett. **65** (1997) 615 [hep-ph/9704255].
[43] K. J. Eskola, H. Honkanen, C. A. Salgado and U. A. Wiedemann, Nucl. Phys. **A747** (2005) 511 [hep-ph/0406319]; A. Dainese, C. Loizides and G. Paic, Eur. Phys. J. **C38** (2005) 461 [hep-ph/0406201].
[44] A. H. Rezaeian and Z. Lu, Nucl. Phys. **A826** (2009) 198 [arXiv:0810.4942]; B. Z. Kopeliovich, A. H. Rezaeian, I. Schmidt, Phys. Rev. **D78** (2008) 114009 [arXiv:0809.4327].
[45] For a review see: D. d'Enterria, Landolt-Boernstein Vol. 1-23A (Springer Verlag), arXiv:0902.2011.
[46] F. Dominguez, C. Marquet, A. H. Mueller, B. Wu and B. W. Xiao, Nucl. Phys. **A811** (2008) 197 [arXiv:0803.3234].
[47] C. P. Herzog, A. Karch, P. Kovtun, C. Kozcaz and L. G. Yaffe, JHEP **0607** (2006) 013 [hep-th/0605158].
[48] S. S. Gubser, Phys. Rev. **D74** (2006) 126005 [hep-th/0605182].
[49] H. Liu, K. Rajagopal and U. A. Wiedemann, Phys. Rev. Lett. **97** (2006) 182301 [hep-ph/0605178].
[50] M. Gyulassy, P. Levai and I. Vitev, Phys. Rev. Lett. **85** (2000) 5535 [nucl-th/0005032].
[51] M. Gyulassy, P. Levai and I. Vitev, Nucl. Phys. **B594** (2001) 371 [nucl-th/0006010].
[52] M. Gyulassy, I. Vitev, X. N. Wang and B. W. Zhang, Published in Quark Gluon Plasma 3, editors: R. C. Hwa and X. N. Wang, World Scientific, Singapore. In Hwa, R. C. (ed.) *et al.*: Quark gluon plasma, 123-191, nucl-th/0302077.
[53] C. A. Salgado and U. A. Wiedemann, Phys. Rev. **D68** (2003) 014008 [hep-ph/0302184].
[54] Y. L. Dokshitzer, V. A. Khoze, and S. I. Troian, J. Phys. **G17** (1991) 1585; V. A. Khoze, W. Ochs, and J. Wosiek, hep-ph/0009298; V. A. Khoze and W. Ochs, Int. J. Mod. Phys. **A12** (1997) 2949, and reference therein.
[55] D. Kharzeev, E. Levin, M. Nardi and K. Tuchin, Nucl. Phys. **A826** (2009) 230 [arXiv:0809.2933]; Phys. Rev. Lett. **102** (2009) 152301 [arXiv:0808.2954].
[56] K. Tuchin, Phys. Lett. **B593** (2004) 66 [hep-ph/0401022].
[57] Y. V. Kovchegov and K. Tuchin, Phys. Rev. **D74** (2006) 054014 [hep-ph/0603055].
[58] Y. V. Kovchegov, Nucl. Phys. **A692** (2001) 557 [hep-ph/0011252].
[59] B. Z. Kopeliovich, A. V. Tarasov and A. Schäfer, Phys. Rev. **C59** (1999) 1609 [hep-ph/9808378].
[60] B. Z. Kopeliovich and A. H. Rezaeian, Int. J. Mod. Phys. E **18** (2009) 1629 [arXiv:0811.2024] and references therein.
[61] K. J. Golec-Biernat and M. Wusthoff, Phys. Rev. **D60** (1999) 114023 [hep-ph/9903358].
[62] E. Levin and K. Tuchin, Nucl. Phys. **A693** (2001) 787, [arXiv:hep-ph/0101275]; **A691** (2001) 779 [hep-ph/0012167]; **B573** (2000) 833, [hep-ph/9908317].
[63] B. Z. Kopeliovich, I. K. Potashnikova, B. Povh and I. Schmidt, Phys. Rev. **D76** (2007) 094020 [arXiv:0708.3636].
[64] A. Kormilitzin and E. Levin, arXiv:1009.1468.

[65] E. Gotsman, E. Levin, U. Maor and E. Naftali, Nucl. Phys. **A750** (2005) 391 [hep-ph/0411242].
[66] J. L. Albacete and C. Marquet, Phys. Lett. **B687** (2010) 174 [arXiv:1001.1378].
[67] G. Watt and H. Kowalski, Phys. Rev. **D78** (2008) 014016.
[68] K. Golec-Biernat and A. M. Stasto, Nucl. Phys. **B668** (2003) 345; J. Berger and A. Stasto, arXiv:1010.0671.
[69] S. Abreu *et al.*, J. Phys. **G35** (2008) 054001 [arXiv:0711.0974].